0026-895X/90/060893-10$02.00/0

MOLECULAR PHARMACOLOGY, 37:893-902

On the Involvement of Multiple Muscarinic Receptor Subtypes in the Activation of Phosphoinositide Metabolism in Rat Cerebral Cortex

CARLOS FORRAY and ESAM E. EL-FAKAHANY[1]

Department of Pharmacology and Toxicology, University of Maryland School of Pharmacy, Baltimore, Maryland 21201

Received October 9, 1989; Accepted February 7, 1990

SUMMARY

We have examined the activation of phosphoinositide metabolism by muscarinic agonists in rat cerebral cortex, in an attempt to delineate the mechanisms by means of which some selective antagonists inhibit this response in a manner that deviates from simple mass action law. The accumulation of [^{3}H]inositol phosphates induced by the full agonist carbamylcholine in cell aggregates preparations was inhibited by muscarinic antagonists with the following order of potency: telenzepine > atropine > 4-diphenylacetoxy-*N*-methyl-piperidine methbromide > pirenzepine > hexahydro-sila-difenidol > AF-DX 116. The same order of potency was found for the competition of these antagonists with [^{3}H]telenzepine binding to M_1 muscarinic receptors. The inhibition of the formation of [^{3}H]inositol phosphates activated by acetylcholine, carbamylcholine, and oxotremorine-M by pirenzepine and telenzepine showed biphasic curves, with 62–73% of the response being inhibited with high affinity. Atropine, AF-DX 116, and pirenzepine shifted the concentration-response curves of oxotremorine-M to the right in a parallel manner. However, pirenzepine at micromolar concentrations showed deviation from linearity of the Schild regression. The blockade by high concentrations of pirenzepine and telenzepine showed less than additive dose ratios when assayed in the presence of atropine, suggesting deviation of their antagonism from simple competition. However, after alkylation with propylbenzilylcholine mustard in the presence of low concentrations of pirenzepine, the response to carbamylcholine and oxotremorine-M showed monophasic inhibition curves by pirenzepine and linear Schild regression for this antagonist. These results support the interpretation that the formation of [^{3}H]inositol phosphates is activated by multiple muscarinic receptor subtypes in rat cerebral cortex. The profile of affinities of muscarinic antagonists indicates that a major component of the response is activated by an M_1 receptor subtype and a minor component is probably mediated by M_3 muscarinic receptors when acetylcholine, carbamylcholine, or oxotremorine-M are used to stimulate the response. Conversely, pirenzepine inhibited the response induced by methacholine and bethanechol in a monophasic manner with high affinity (K_i = 13 nM), suggesting that these agonists can selectively stimulate phosphoinositide metabolism through activation of M_1 muscarinic receptors in rat cerebral cortex.

The actions of acetylcholine as a neurotransmitter in the central and peripheral nervous system are largely mediated by muscarinic receptors, which have been found to display considerable heterogeneity at the functional level. Selective antagonists interact with muscarinic receptors with differing affinities and have been instrumental in the differentiation of muscarinic receptor subtypes (1). It initially became evident that heart muscarinic receptors could be distinguished from those present in peripheral ganglia by differential affinity for the antagonist pirenzepine, leading to the classification of muscarinic receptors into M_1 and M_2 subtypes (2). It also became apparent that antagonist selectivity could discriminate between the coupling of different muscarinic receptor subtypes to specific cellular effectors, such as the inhibition of cyclic AMP formation, activation of cyclic GMP synthesis, and activation of inositol lipid metabolism (3–5), suggesting that the functional heterogeneity of muscarinic receptors is closely associated with their pharmacological classification. Later, the pharmacological profile derived from the selectivity of antagonists in binding to muscarinic receptors in hippocampus, atrium, and submandibular glands led to the subclassification of the receptors with low affinity for pirenzepine into M_2 and M_3, in order to accommodate a subset of receptors (M_3) that showed an intermediate

This work was supported by National Institutes of Health Grants NS-24158, NS-25743, and AG-07118 and by contract DAAL-03-88-0078 from the United States Army Research Office.

[1] Recipient of a Research Career Development Award from the National Institutes of Health (AG-00344).

ABBREVIATIONS: AF-DX 116, (11-{2-[(diethylamino)-methyl]-1-piperidinyl}acetyl)-5,11-dihydro-6*H*-pyrido(2,3-*b*)(1,4)benzodiazepin-6-one; [^{3}H]NMS, [N-methyl-^{3}H]scopolamine methyl chloride; HHSiD, hexahydro-sila-difenidol; 4-DAMP, 4-diphenylacetoxy-*N*-methyl-piperidine methbromide; EC_{50}, concentration of agonist required to elicit 50% maximal response; IC_{50}, concentration of antagonist necessary to inhibit 50% of agonist response; K_b or K_i, antagonist dissociation constant; PI, phosphoinositide; PBCM, propylbenzilylcholine mustard; KH, Krebs-Henseleit; A-S Arunlakshana-Schild.

affinity for pirenzepine and low affinity for the cardioselective antagonist AF-DX 116 (6). Thus, there are currently three muscarinic receptor subtypes that have been defined pharmacologically.

In recent years, the cloning of five different muscarinic receptor genes has provided new insights into the possible basis for receptor heterogeneity (7–11). The encoded receptor proteins show pharmacological profiles (7–9, 12) and tissue distributions of the corresponding mRNA (13–15) that correlate closely with the pharmacological classification of muscarinic receptors. These findings seem to indicate that, to a great extent, the basis for receptor heterogeneity resides in the primary structure of the receptor protein. In addition, the transfection of cultured cells with the cloned muscarinic receptor genes has shown that the expressed sequences show preferential coupling to different effectors (16–18). Brain muscarinic cholinergic receptors have been consistently found to activate PI metabolism (19–22). The initial finding that this response in rat brain was inhibited with high affinity by pirenzepine led to the conclusion that it was activated through an M_1 muscarinic receptor subtype (3). This is in contrast to the activation of this response by muscarinic agonists in glandular tissue, where it was found to be inhibited by pirenzepine with a 6- to 7-fold lower potency (3). Besides the differences observed with selective antagonists, it was also evident that muscarinic agonists differ in their potency and efficacy in the activation of the PI response in glandular and brain tissue (3, 22). These data indicated that PI metabolism can be mediated by the M_1 as well as the M_3 muscarinic receptor subtype. Waelbroek and coworkers (23, 24) found evidence consistent with the presence of three distinct muscarinic receptor populations in rat brain, on the basis of kinetic studies with ^{3}H-ligands. Moreover, as a result of *in situ* hybridization studies, mRNAs encoding these three receptor subtypes have been found in rat brain (13, 14). Furthermore, expressed m1, m3, and m5 muscarinic receptor gene products can activate PI metabolism (10, 11, 16–18), giving support to the contention that there is more than one receptor subtype that can couple to this effector system.

Studies of muscarinic receptor-mediated activation of PI metabolism in rat brain cortex (25–27) and striatum (28) indicated that pirenzepine inhibited this response with more than one affinity, based on the shallow inhibition curves of the response by this antagonist. Moreover, it was also found that the PI response of the guinea pig neostriatum and brainstem is inhibited by pirenzepine with much lower potency than that in the hippocampus or cerebral cortex (22). Taken together, these data suggest that the stimulation of PI metabolism in brain tissue could be the result of activation of more than one muscarinic receptor subtype. However, the pharmacological nature of the component of the response that is blocked by pirenzepine with low affinity has not been elucidated. The present study of muscarinic receptor-mediated PI metabolism in rat cerebral cortex was designed with several goals, as follows: first, to distinguish the contribution of multiple muscarinic receptor subtypes in eliciting the PI response from other potential complicating mechanisms (e.g., cooperative interaction of pirenzepine with muscarinic receptors); second, to pharmacologically define the muscarinic receptor subtypes involved by using a group of selective antagonists; and finally, to investigate the possible selectivity of muscarinic agonists in activating the PI response through multiple receptor subtypes in the rat cerebral cortex.

Experimental Procedures

Materials. HHSiD was a gift of Dr. G. Lambrecht at the University of Frankfurt. AF-DX 116 and pirenzepine were supplied by Boehringer Ingelheim Pharmaceuticals, Inc. (Ridgefield, CT). Telenzepine was supplied by Byk Gulden Pharmaceuticals (Konstanz, FRG). 4-DAMP was a gift of Dr. R. B. Barlow at the University of Bristol. Oxotremorine-M was purchased from Research Biochemicals Inc. (Natik, MA). McN-A-343 was obtained from McNeil Laboratories (Springhouse, PA). Carbamylcholine, atropine, bethanechol, arecoline, pilocarpine, methacholine, muscarine, and acetylcholine were purchased from Sigma Chemical Co. (St. Louis, MO). Dowex-1-X8 resin (100–200 mesh) was purchased from Bio-Rad (Rockville Center, NY). *myo*-[^{3}H]Inositol (82.5 Ci/mmol) was purchased from Amersham (Arlington Heights, IL). [^{3}H]NMS (84.8 Ci/mmol), [^{3}H]telenzepine (70.2 Ci/mmol), and PBCM were purchased from New England Nuclear (Boston, MA).

Preparation of cell aggregates. This tissue preparation, originally described by Honegger and Richelson (29) for the dissociation of fetal brain tissue for primary culture purposes, has been modified to obtain an intact brain cell preparation for receptor binding as well as functional assays and has been described in detail elsewhere (5, 30). Briefly, the cerebral cortex from adult male Sprague-Dawley rats was dissected over an ice-cold surface, finely minced, and suspended in ice-cold modified Puck's D1 solution (138 mM NaCl, 5.4 mM KCl, 0.17 mM Na_2HPO_4, 0.22 mM KH_2PO_4, 5.5 mM glucose, 58.4 mM sucrose; adjusted to pH 7.4 and 340 mOsm). The cell aggregates were obtained by forcing the minced tissue through a nylon mesh bag (210-μm pore; Nitex), followed by filtration through a second nylon mesh bag (130-μm pore; Nitex). The preparation was washed twice by centrifugation (400 × *g* for 1 min at 4°), suspended in modified KH buffer (118 mM NaCl, 4.7 mM KCl, 1.2 mM KH_2PO_4, 1.3 mM $CaCl_2$, 1.2 mM $MgSO_4$, 1.2 mM glucose, 25 mM $NaHCO_3$), and preincubated at 37° under 95% O_2/5% CO_2 for 20 min.

Assay of inositol phosphates accumulation. After preincubation in KH buffer, cell aggregates were centrifuged, suspended in fresh buffer containing 15 μCi/ml *myo*-[^{3}H]inositol, and incubated at 37° under 95% O_2/5% CO_2 for 60 min. The preparation was then centrifuged to eliminate unincorporated radioactivity and suspended in KH buffer containing 10 mM LiCl. The labeled cell aggregates were incubated at 37° under 95% O_2/5% CO_2 in the presence of antagonists for 20 min before the addition of the agonist, in a final volume of 0.4 ml. The reaction was stopped after 60 min with 1 ml of $CHCl_3$/methanol/concentrated HCl (2:1:0.01, v/v), and then 0.25 ml of water containing 1500 dpm of [^{14}C]inositol-1-phosphate was added to correct for losses during the isolation procedure. The [^{3}H]inositol phosphates formed were isolated by ion exchange chromatography of the aqueous phase on Dowex 1-X8 (formate form), as described by Berridge *et al.* (31). After washes with water and 60 mM ammonium formate, 5 mM sodium borate, total [^{3}H]inositol-phosphates were eluted with 1 M ammonium formate, 0.1 M formic acid. The radioactivity from ^{3}H and ^{14}C in this fraction was determined by liquid scintillation counting and corrected individually for counting efficiencies and recovery. The organic phase from each sample was evaporated, counted to determine the radioactivity incorporated into the lipid fraction, and used to express the data as a percentage of conversion of [^{3}H]inositol phospholipids into [^{3}H]inositol phosphates.

Binding assays. Suspensions of cell aggregates in KH buffer were incubated in the presence of either 0.2 nM [^{3}H]NMS or 1 nM [^{3}H]telenzepine. Incubations were carried out at 37° in an atmosphere of 95% O_2/5% CO_2 for 3 hr. Nonspecific binding was measured in the presence of 2 μM atropine. The incubations were terminated by filtration of the samples through GF/B glass fiber filters, followed by washings with ice-cold 0.9% NaCl, using a cell harvester (Skatron,

Norway). Radioactivity retained on the filters was determined by liquid scintillation counting and corrected individually for counting efficiency.

Alkylation experiments. Muscarinic receptors in cell aggregate preparations were alkylated by incubation with 30 nM PBCM. The mustard was cyclized by incubation in 5 mM phosphate buffer (pH 7.0) for 20 min before its addition to the cell aggregates preparation. In experiments in which M_1 muscarinic receptors were protected from alkylation, cell aggregates were incubated with 50 nM pirenzepine for 20 min before the cyclized mustard was added. The alkylation reaction was stopped by dilution of the incubation mixture in 10 volumes of ice-cold KH buffer, followed by low speed centrifugation. This procedure was repeated two more times before either labelling of the preparation with *myo*-[^{3}H]inositol for functional assays or addition of the labelled ligands for binding assays.

Data analysis. Data from concentration-response curves were fitted untransformed to a four parameter logistic function by means of nonlinear regression analysis, using the GraphPAD computer program (ISI, Philadelphia, PA) which gave estimates of the basal level, maximum response, EC_{50}, and slope of the curve. Dose ratios for Arunlakshana-Schild regressions (32) were calculated from the ratios between the EC_{50} values, estimated by the nonlinear regression analysis, in the presence and absence of antagonists. Experiments in which the effects of a single concentration of agonist were assayed in the presence of varying concentrations of antagonists were analyzed as competition curves by nonlinear regression analysis for models of one or two noninteracting sites. IC_{50} values were converted to antagonist dissociation constants (K_b), applying the equation $K_b = IC_{50}/(1+[\text{agonist}]/EC_{50})$ (33). The goodness of fit of the data to a two versus one site model was estimated by the F test of the sum of squares of residuals from both fittings, using a criterion of significance of $p < 0.05$. The data from binding experiments were analyzed by nonlinear regression analysis, using the LIGAND computer program (34).

Results

Formation of [^{3}H]inositol phosphates by muscarinic agonists. Incubation of cortical cell aggregates with 1 mM carbamylcholine in the presence of 10 mM LiCl induced a maximal accumulation of [^{3}H]inositol phosphates between 4- and 6-fold over basal values (basal = 3860 ± 220 dpm, 70 experiments). When different muscarinic agonists were added to cell aggregate preparations at maximally effective concentrations, it was apparent that bethanechol, arecoline, pilocarpine, oxotremorine, and McN-A-343 were unable to stimulate the formation of [^{3}H]inositol phosphates to the same extent as acetylcholine (Fig. 1). There were no statistically significant differences between acetylcholine, carbamylcholine, oxotremorine-M, methacholine, and muscarine in their efficacy in activating the PI response. Concentration-response curves for the formation of [^{3}H]inositol phosphates by muscarinic agonists showed the following order of potency: oxotremorine-M > acetylcholine > methacholine > carbamylcholine > bethanechol. The slope factors of the concentration-response curves were close to unity for all the agonists (Table 1).

Antagonism of muscarinic receptor-mediated formation of [^{3}H]inositol phosphates. After equilibration of rat cerebral cortex cell aggregates with concentrations of pirenzepine varying from 10^{-9} to 10^{-4} M, the formation of [^{3}H]inositol phosphates was activated by 1 mM carbamylcholine for 60 min in the presence of 10 mM LiCl. Inhibition curves were shallow, with Hill coefficients consistently smaller than 1 (Fig. 2; Table 2). These curves were better fitted to a two-site competition model and the pK_b values of pirenzepine at both sites were derived, assuming that carbamylcholine activated the response at both sites with the same EC_{50}. Two thirds of the carbamylcholine-induced [^{3}H]inositol phosphate formation was inhibited by pirenzepine with high affinity (8 nM) and the remainder of the response was inhibited with a 30-fold lower affinity. When acetylcholine (Fig. 3) or oxotremorine-M was used to activate the formation of [^{3}H]inositol phosphates in cell aggregates, the resulting inhibition curves were virtually identical to those of carbamylcholine (Fig. 2; Table 3). However, when either methacholine or bethanechol was employed, the resulting inhibition curves were monophasic and were best fitted to a one-site model with high affinity for pirenzepine (Fig. 3; Table 3).

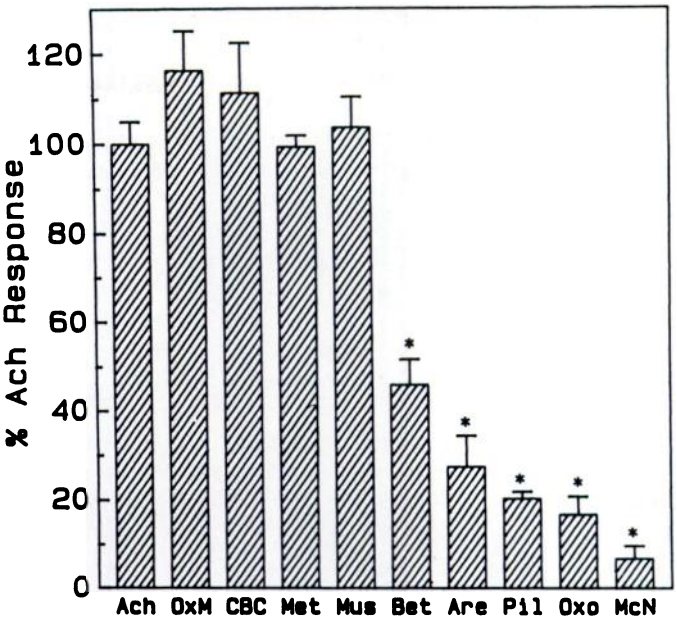

Fig. 1. Activation of [^{3}H]inositol phosphates accumulation in rat cerebral cortex by various muscarinic agonists. Cell aggregates were prepared and labeled as described in Experimental Procedures and suspended in KH buffer containing 10 mM LiCl. Then, cells were stimulated for 60 min with 0.1 mM acetylcholine (*Ach*), 0.1 mM oxotremorine-M (*OxM*), 0.1 mM oxotremorine (*Oxo*), 1 mM carbamylcholine (*CBC*), 1 mM methacholine (*Met*), 1 mM muscarine (*Mus*), 1 mM bethanechol (*Bet*), 1 mM arecoline (*Are*), 1 mM pilocarpine (*Pil*), or 1 mM McN-A-343 (*McN*). Date are mean ± standard error from three independent experiments performed in triplicate. *$p < 0.05$ versus acetylcholine (one-way analysis of variance).

TABLE 1

Muscarinic agonists stimulation of [^{3}H]inositol phosphates accumulation in rat brain cortex cell aggregates.

Cell aggregates were prepared, labeled for 60 min with *myo*-[^{3}H]inositol, and exposed to the different agonists for another 60 min in the presence of 10 mM LiCl. Results are shown as the percentage of conversion over basal, and the estimation of the parameters from concentration-response curves was performed as described in Experimental Procedures. The concentrations of agonists used to construct the concentration response curves were 100 nM to 1 mM for acetylcholine and oxotremorine-M and 1 μM to 10 mM for carbamylcholine, methacholine, and bethanechol. The unstimulated level of conversion to inositol phosphates was 28 ± 0.53% (32 experiments). Values shown are the mean ± standard error for 3 to 10 independent experiments.

Agonist	EC_{50}	Slope	E_{max} (% Conversion)
	μM		
Acetylcholine[a]	14 ± 2	0.9 ± 0.1	52 ± 1.9
Oxotremorine-M	9 ± 1	1.0 ± 0.1	55 ± 3.3
Carbamylcholine	173 ± 22	1.0 ± 0.2	55 ± 1.1
Methacholine[a]	66 ± 8	0.9 ± 0.1	57 ± 0.8
Bethanechol	258 ± 31	0.9 ± 0.2	39 ± 0.9[b]

[a] Determined in the presence of 10 μM physostigmine.
[b] $p < 0.05$ versus all the other agonists.

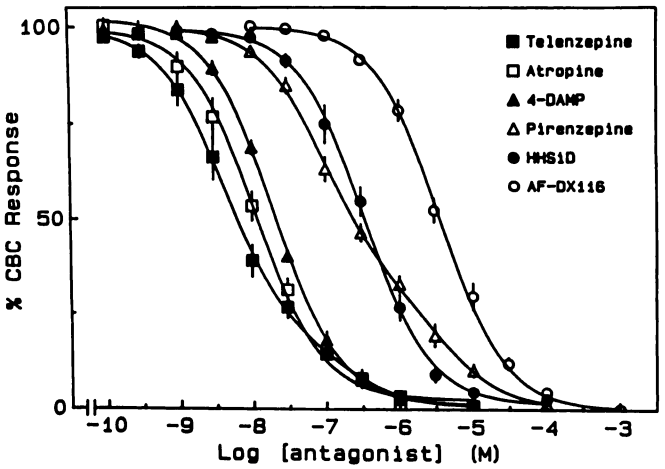

Fig. 2. Inhibition of carbamylcholine-stimulated [^{3}H]inositol phosphates by muscarinic antagonists in rat cerebral cortex. Cell aggregates were prepared and labeled as described in Experimental Procedures, suspended in KH buffer containing 10 mM LiCl, and equilibrated with antagonists for 20 min. Then, 1 mM carbamylcholine was added and incubated for 60 min. Data are expressed as a percentage of the response induced by carbamylcholine in the absence of antagonist and are shown as mean ± standard error from at least four independent experiments, performed in triplicate. *CBC*, carbamylcholine.

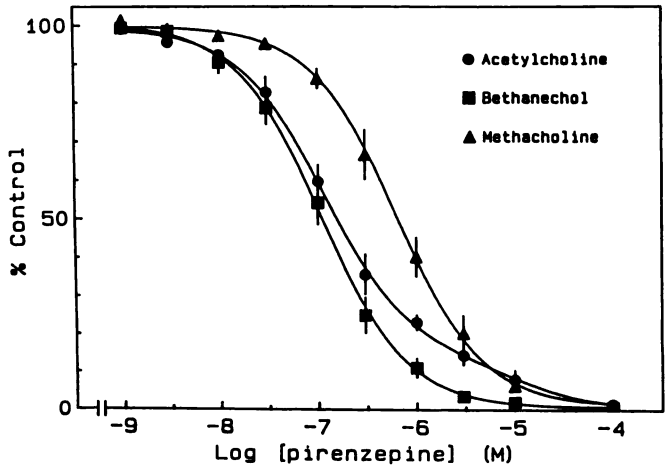

Fig. 3. Inhibition by pirenzepine of [^{3}H]inositol phosphates accumulation induced by muscarinic agonists in rat cerebral cortex. Cell aggregates were prepared and labeled as described in Experimental Procedures, suspended in KH buffer containing 10 mM LiCl, and equilibrated with pirenzepine for 20 min. Then, 0.1 mM acetylcholine, 3 mM methacholine, or 3 mM bethanechol were added and incubated for 60 min. Acetylcholine and methacholine were assayed in the presence of 10 μM physostigmine. Data are expressed as a percentage of stimulation by the agonist in the absence of antagonist and are representative of at least four experiments, each performed in triplicates.

TABLE 2

Inhibition by muscarinic antagonists of the accumulation of [^{3}H] inositol phosphates induced by carbamylcholine

Values were derived from nonlinear regression analysis (described in Experimental Procedures) of the competition curves shown in Fig. 2. Data are shown as the mean ± standard error of n independent experiments. pK_h and pK_l are the negative logarithms of high and low affinity dissociation constants. R_h (%) is the percentage of receptors exhibiting high affinity and n_H is the Hill coefficient.

Antagonist	n	pK_h	pK_l	R_h	n_H
				%	
Pirenzepine	8	8.10 ± 0.05	6.58 ± 0.13	62 ± 3	0.7 ± 0.02
Telenzepine	7	8.90 ± 0.08	6.63 ± 0.32	73 ± 3	0.7 ± 0.03
AF-DX 116	6	6.12 ± 0.28		100	1.0 ± 0.06
HHSiD	4	7.48 ± 0.04		100	1.0 ± 0.03
4-DAMP	4	8.62 ± 0.03		100	0.9 ± 0.04
Atropine	4	9.02 ± 0.13		100	0.9 ± 0.10

TABLE 3

Inhibition by pirenzepine of the accumulation of [^{3}H]inositol phosphates induced by muscarinic agonists in cell aggregates from rat cerebral cortex

Cell aggregates were incubated for 20 min at 37° with pirenzepine concentrations ranging from 1×10^{-9} to 1×10^{-4} M in the presence of 10 mM LiCl, then a fixed concentration of the agonist was added (0.1 mM acetylcholine and oxotremorine-M and 1 mM carbamylcholine, methacholine, and bethanechol), and the reaction was stopped 60 min later. The results shown are the mean ± standard error of the estimates obtained by nonlinear regression analysis from n independent experiments, each performed in triplicate. See Table 2 for abbreviations.

Agonist	n	pK_h	pK_l	R_h
				%
Carbamylcholine	8	8.10 ± 0.05	6.58 ± 0.13	62 ± 3
Acetylcholine*	4	8.07 ± 0.11	6.56 ± 0.16	75 ± 5
Oxotremorine-M	4	7.86 ± 0.09	6.51 ± 0.06	81 ± 5
Methacholine*	4	7.89 ± 0.11		100
Bethanechol	4	7.90 ± 0.10		100

* Assayed in the presence of 10 μM physostigmine.

The inhibition of the carbamylcholine-activated formation of [^{3}H]inositol phosphates by telenzepine also yielded a multiphasic inhibition curve, with 70% of the response being inhibited with a potency 10-fold higher than that of pirenzepine (Fig. 2; Table 2). However, inhibition of the response of other muscarinic antagonists resulted in monophasic inhibition curves, with a rank order of potencies of atropine > 4-DAMP > HHSiD > AF-DX 116 (Fig. 2; Table 2).

Because pirenzepine and telenzepine were the only antagonists that showed inhibition curves with Hill coefficients less than 1, concentration-response curves of oxotremorine-M were obtained at different concentrations of pirenzepine (see legend to Fig. 4) in order to compare the resulting A-S plot with that of the nonselective antagonist atropine and of AF-DX 116, an antagonist with the opposite selectivity of pirenzepine. Oxotremorine-M was chosen because its higher potency would permit assay of a wider range of concentrations of pirenzepine. As shown in Fig. 4, pirenzepine induced a parallel displacement of the concentration-response curve at all concentrations assayed. However, at concentrations of pirenzepine above 1 μM, the magnitude of the rightward shift of the concentration-response curves was decreased. Linear regression analysis of these data showed a slope of 0.83 ± 0.05 with an apparent pA_2 of 8.03, which became 7.93 after the slope was constrained to unity. The A-S plots for atropine and AF-DX 116 yielded slopes of 0.91 and 0.96, with pA_2 values of 8.82 and 6.23, respectively (Fig. 5). In contrast, when methacholine was used instead of oxotremorine-M, the resulting A-S plot for pirenzepine showed no deviation from linearity, with a slope of 0.97 ± 0.03 and a pA_2 of 7.66 (Fig. 6).

To further characterize the behavior of pirenzepine and telenzepine at high concentrations, the additivity of the shifts in the concentration-response curves caused by each of these two antagonists with an equal shift induced by atropine was studied. As shown in Table 4, the dose ratios of the combination of 100 nM pirenzepine or 10 nM telenzepine with 10 nM atropine were additive when compared with the sum of the dose ratios obtained by addition of each antagonist separately, suggestive of competitive interaction. However, at 5-fold higher concentrations of pirenzepine and telenzepine, the additivity of the

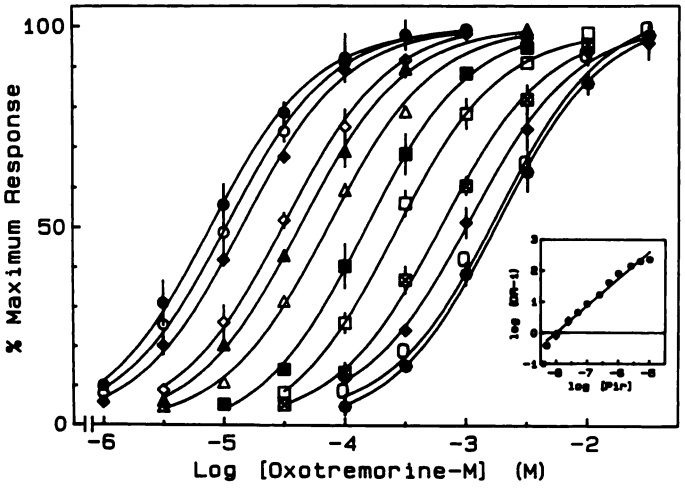

Fig. 4. Schild analysis of the antagonism by pirenzepine of oxotremorine-M-stimulated accumulation of [^{3}H]inositol phosphates in rat cerebral cortex. Cell aggregates were prepared and labeled as described in Experimental Procedures, suspended in KH buffer containing 10 mM LiCl, and equilibrated without (●) or with 5 nM (○), 10 nM (♦), 25 nM (◇), 50 nM (▲), 100 nM (△), 250 nM (■), 500 nM (□), 1 μM (⊠), 2.5 μM (⊕), 5 μM (⊡), or 10 μM (⊕) pirenzepine for 20 min. The formation of [^{3}H]inositol phosphates was then activated with increasing concentrations of oxotremorine-M. Data are shown as mean ± standard error of three independent experiments, each performed in triplicate. *Inset*, Schild plot. Dose ratios (*DR*) were determined from the EC_{50} values estimated from nonlinear regression analysis of the concentration-response curves. The resulting Schild plot was fitted to linear regression analysis that estimated a slope value of 0.86 ± 0.04, with an apparent pA_2 of 8.0.

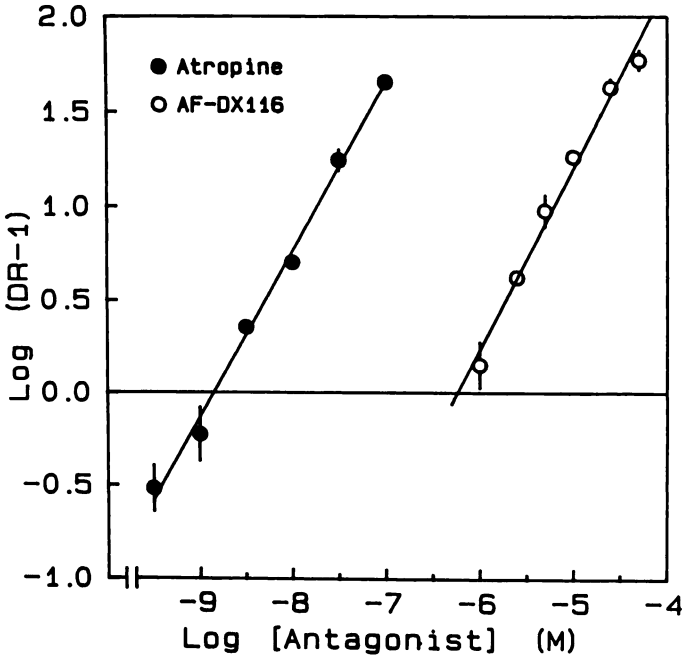

Fig. 5. Schild regressions of the antagonism by atropine and AF-DX 116 of [^{3}H]inositol phosphates formation by oxotremorine-M in rat cerebral cortex. Cell aggregates were prepared and labeled as described in Experimental Procedures, suspended in KH buffer containing 10 mM LiCl, and incubated for 20 min in the presence of the antagonists. Oxotremorine-M was then added and incubated for 60 min. Dose ratios (*DR*) were determined from EC_{50} values estimated from nonlinear regression analysis of concentration-response curves constructed with seven concentrations of oxotremorine-M at each concentration of antagonist. Data are shown as mean ± standard error of three independent experiments, each performed in triplicate. The estimated pA_2 values are 8.82 and 6.23, with slopes of 0.91 and 0.96 for atropine and AF-DX 116, respectively.

dose ratios with that produced by 30 nM atropine was lost (Table 4).

In order to distinguish the presence of receptor heterogeneity from a possible allosteric behavior of pirenzepine and telenzepine, we designed experiments in which the sites that bind pirenzepine with high affinity were selectively protected against receptor alkylation by PBCM. Cortical cell aggregates were incubated to equilibrium with or without 50 nM pirenzepine, then 30 nM activated mustard was added, and the reaction was stopped by dilution of the mustard at different time points. This concentration of pirenzepine should saturate approximately 85% of the high affinity receptors and less than 5% of the low affinity ones. As shown in Fig. 7, the specific binding of [^{3}H]NMS decayed at a slower rate in the presence of 50 nM pirenzepine, with a maximal protection at 4 min. Thus, this time point was selected and used for treatment of cell aggregate preparations before assay of the activation of the PI response by carbamylcholine. The concentration-response curve for carbamylcholine after alkylation in the presence of 50 nM pirenzepine showed a 45% reduction of the maximal response, with no change in the EC_{50} (223 ± 12 versus 245 ± 25 μM) (Fig. 8). Moreover, the pirenzepine inhibition curve after selective alkylation showed a significantly better fit to a one-site model, with a pK_b of 7.87 and a Hill coefficient of 0.93 ± 0.05 (Fig. 9), indicating that in cell aggregates treated in this manner the PI response is mediated by a single receptor class to which pirenzepine binds with high affinity. Furthermore, after protected alkylation, the regression line of the A-S plot using oxotremorine-M as an agonist showed no deviation from linearity up to 10 μM pirenzepine, with a slope of 0.95 ± 0.03 and an estimated pA_2 value of 7.96 (Fig. 10).

Binding experiments. The equilibrium dissociation con-

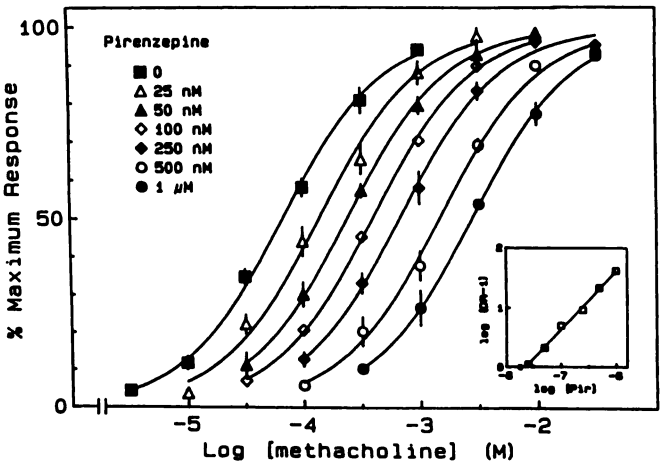

Fig. 6. Schild analysis of the antagonism by pirenzepine of [^{3}H]inositol phosphates formation induced by methacholine in rat cerebral cortex. Cell aggregates were prepared and labeled as described in Experimental Procedures and were suspended in KH buffer containing 10 mM LiCl and 10 μM physostigmine. Then, the indicated concentrations of pirenzepine were added and cells were incubated for 20 min. The formation of [^{3}H] inositol phosphates was stimulated with seven doses of methacholine for each concentration of pirenzepine, for 60 min. Data are shown as mean ± standard error from three independent experiments, each performed in triplicate. *Inset*, Schild plot. Dose ratios (*DR*) were calculated from the EC_{50} values obtained by nonlinear regression analysis of the concentration-response curves. The linear regression analysis of the data estimated a slope of 0.97 ± 0.03, with a pA_2 of 7.66.

TABLE 4

Test for additivity of the dose ratios (DR) of pirenzepine and telenzepine in the presence and absence of atropine

Cell aggregates were prepared and labeled with *myo*-[^{3}H]inositol as described under Experimental Procedures and incubated in KH buffer containing 10 mM LiCl with the indicated concentrations of antagonists for 20 min, and the formation of [^{3}H]inositol-phosphates was stimulated with oxotremorine-M for 60 min. Concentration-response curves were constructed and the EC_{50} values were estimated by nonlinear regression analysis. Data are shown as the mean ± standard error from three independent experiments. The EC_{50} for oxotremorine-M in the absence of antagonists was 6.6 ± 2 μM.

Antagonist	Experimental DR-1	Theoretical DR-1[a]
Pirenzepine, 100 nM	7 ± 0.7	
Telenzepine, 10 nM	8 ± 0.5	
Atropine, 10 nM	8 ± 0.4	
Pirenzepine + Atropine	17 ± 1.6	15
Telenzepine + Atropine	15 ± 0.2	16
Pirenzepine, 500 nM	32 ± 3.5	
Telenzepine, 50 nM	37 ± 3.3	
Atropine, 30 nM	33 ± 4.0	
Pirenzepine + Atropine	48 ± 4.9	67[b]
Telenzepine + Atropine	52 ± 5.5	73[b]

[a] $DR = DR_{antagonist} + DR_{atropine} - 1$.
[b] $p < 0.05$ versus experimental.

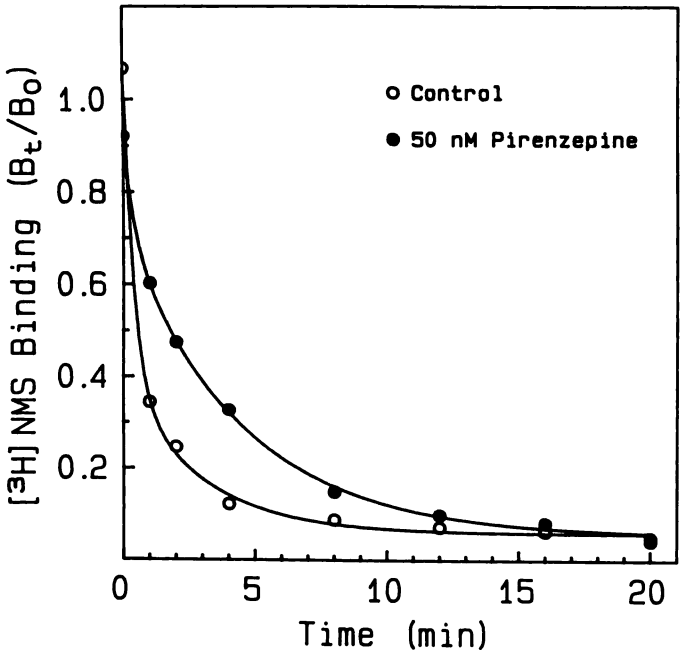

Fig. 7. Rate of alkylation by PBCM of muscarinic receptors in cell aggregate preparations from rat cerebral cortex. Cell aggregates were prepared as described in Experimental Procedures, suspended in KH buffer, and incubated in the absence (○) or presence (●) of 50 nM pirenzepine for 30 min. Then 30 nM PBCM was added and the reaction was stopped at the indicated times. Specific binding of 0.2 nM [^{3}H]NMS was determined as described in Experimental Procedures. Data are the average of triplicate determinations from one representative experiment replicated three times with similar results.

stants of the antagonists used in functional experiments were determined in cell aggregate preparations from rat cerebral cortex, using [^{3}H]NMS. As shown in Table 5, only pirenzepine, telenzepine, and AF-DX 116 showed competition curves with Hill coefficients less than 1. Fitting of these curves to a two-site model estimated a similar proportion of high affinity sites for these three antagonists. Conversely, the competition curves of HHSiD, 4-DAMP, and atropine were consistently monophasic, suggestive of displacement of the labeled ligand with a

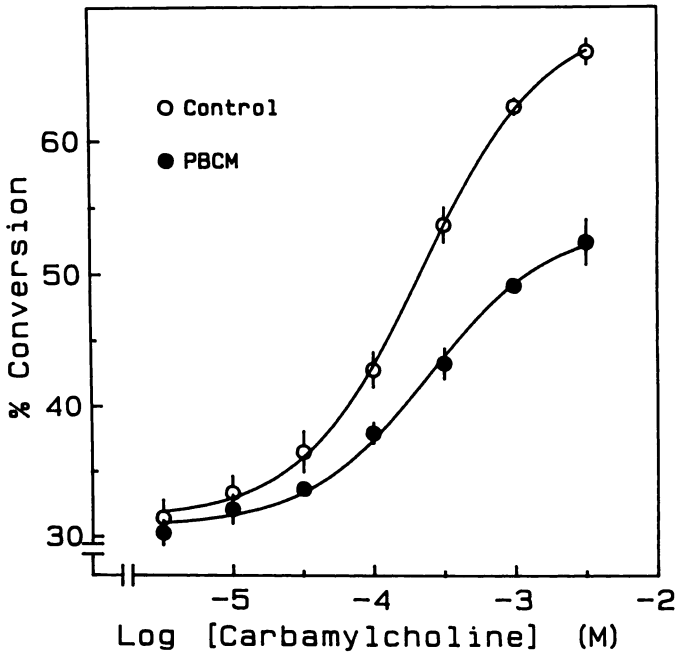

Fig. 8. Effects of selective alkylation of pirenzepine low affinity sites on the concentration-response curves of the activation of [^{3}H]inositol phosphates by carbamylcholine in rat cerebral cortex. Cell aggregates were prepared, suspended in KH buffer, and incubated for 30 min in the presence of 50 nM pirenzepine, and then 30 nM PBCM (●) or 5 mM phosphate buffer (control) (○) was added and the reaction was stopped 4 min later. Then, the preparations were labeled, suspended in KH buffer containing 10 mM LiCl as described in Experimental Procedures, and stimulated by increasing concentrations of carbamylcholine. Data are shown as the mean ± standard error from three independent experiments, each performed in triplicate. EC_{50} values were 223 ± 12 and 245 ± 25 μM for control and PBCM-treated cells, respectively.

similar affinity from all the receptor sites. In fact, a two-site analysis of these curves did not significantly improve the fit.

To allow a direct comparison of the potencies of the antagonists at the muscarinic receptors that show high affinity for pirenzepine, the equilibrium dissociation constants of the antagonists used in the functional assays were determined in cell aggregate preparations, using [^{3}H]telenzepine as a ligand to label M_1 receptors. All the antagonists showed monophasic competition curves, with Hill coefficients close to 1 (Table 6). These antagonists competed against [^{3}H]telenzepine with pK_i values virtually identical to those shown for their high affinity component (or overall affinity) in inhibiting PI hydrolysis (Fig. 11). There was also a positive correlation ($r = 0.98$; slope = 1.04) between the high affinity pK_b values of muscarinic antagonists in inhibiting the PI response induced by carbamylcholine (Table 2) and their high affinity pK_i against [^{3}H]NMS binding (Table 4), with the exception of AF-DX 116, in which case the low affinity pK_i (6.02) was used in the calculations.

Discussion

Activation of PI metabolism by muscarinic agonists in cell aggregates from rat brain cortex showed a profile of potencies and relative efficacies similar to that shown earlier in brain slice preparations (19). Inhibition of the PI response stimulated with the full agonist carbamylcholine by 4-DAMP, HHSiD, and AF-DX 116 resulted in monophasic curves, with pK_b values that correlated closely with their dissociation constants in competing for [^{3}H]telenzepine binding (Fig. 11). The applied

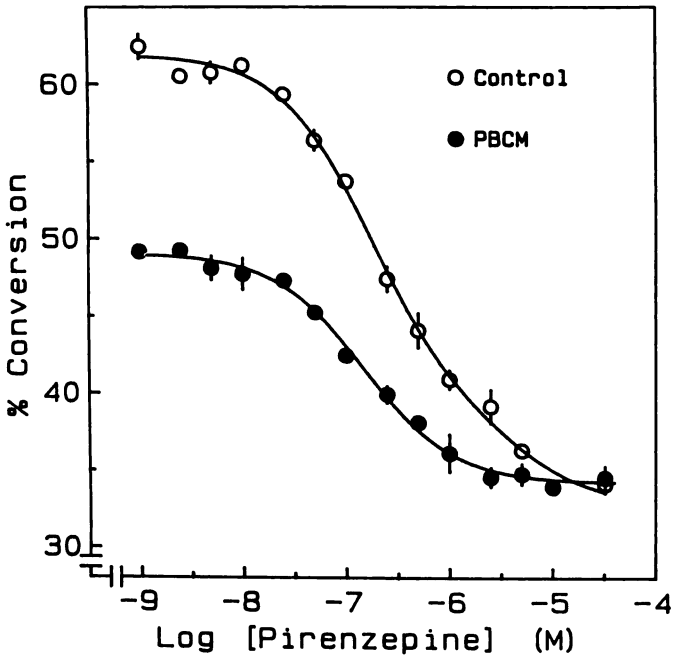

Fig. 9. Effects of selective alkylation of pirenzepine low affinity sites on the inhibition by pirenzepine of carbamylcholine-induced activation of [^{3}H] inositol phosphates in rat cerebral cortex. Cell aggregates were prepared and incubated with 50 nM pirenzepine for 30 min, 30 nM PBCM (●) or 5 mM phosphate buffer (control (○) was added, and the reaction was stopped 4 min later, as described in Experimental Procedures. After incubation for 1 hr with *myo*-[^{3}H]inositol, cell aggregates were suspended in KH buffer containing 10 mM LiCl and were incubated with different concentrations of pirenzepine for 20 min. Then [^{3}H]inositol phosphates accumulation was activated by 1 mM carbamylcholine and the reaction was stopped 60 min later. Data are shown as mean ± standard error from a representative experiment performed in triplicate. Curves represent the nonlinear regression fit to a two site (control, pK_h = 7.81, pK_l = 6.42, and R_h = 67%) and one site (PBCM, pK_i = 7.87) competition models.

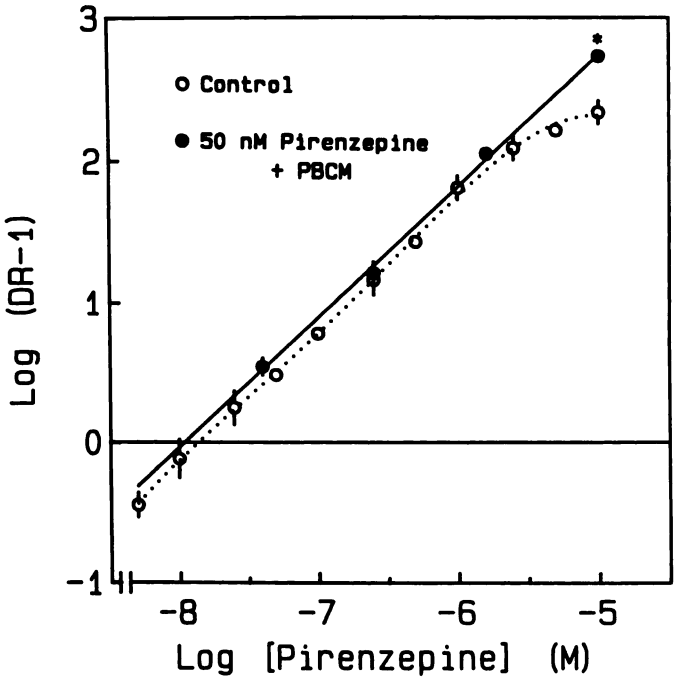

Fig. 10. Schild regression of the antagonism by pirenzepine of the activation of [^{3}H]inositol phosphates by oxotremorine-M after selective alkylation of pirenzepine low affinity sites in rat cerebral cortex. Cell aggregates were prepared and incubated in the presence of 50 nM pirenzepine for 30 min, 30 nM PBCM was added, and the reaction was stopped 4 min later, as described in Experimental Procedures. After labeling, cell aggregates were suspended in KH buffer containing 10 mM LiCl and were incubated for 20 min in the absence or presence of 40 nM, 250 nM, 1.6 μM, or 10 μM pirenzepine. The formation of [^{3}H]inositol phosphates was activated by incubation for 60 min with oxotremorine-M. Dose-ratios (*DR*) were determined from the EC_{50} values estimated by nonlinear regression analysis of concentration-response curves constructed with seven different concentrations of oxotremorine-M. Data are shown as the mean ± standard error from three independent experiments, each performed in triplicate. The slope of the regression line for PBCM-treated cell aggregates is 0.9 ± 0.03 and the pA_2 is 7.96. *Control*, data from Fig. 4, *inset*, plotted here for comparison. *$p < 0.05$ versus control (Student's *t* test).

correction of IC_{50} into K_b values is valid in this case (33), becuase it has been shown that the muscarinic receptors coupled to PI metabolism in rat brain show little receptor reserve (35). Moreover, from the data shown in Fig. 9, a K_a for carbamylcholine of 320 μM (with 43% of receptors blocked) was determined by Furchgott analysis (36). This value is in close agreement with that reported by McKinney *et al.* (5) using the same tissue preparation and lends further support to the notion of a limited receptor reserve for carbamylcholine. In addition, the pA_2 values determined from A-S plots for atropine and AF-DX 116 using oxotremorine-M as an agonist correlated well with the pK_b values determined from inhibition curves of the effect of carbamylcholine and, therefore, give further support to the validity of the analysis. Furthermore, the finding of slope factors close to unity from concentration-response curves suggests that muscarinic agonists are activating the PI response either through a homogeneous population of receptors or with almost identical potency at a heterogeneous receptor population.

When the pK_i values obtained from binding experiments with [^{3}H]telenzepine were compared with those obtained with [^{3}H]NMS as a ligand, 4-DAMP and HHSiD showed similar values and Hill coefficients close to unity in both assays, suggesting that these antagonists show no selectivity towards any of the muscarinic receptor subtypes expressed in rat brain cortex. On the other hand, AF-DX 116 competition curves against [^{3}H]NMS were better modeled to two sites with a 21-fold difference in affinity, in agreement with its high affinity (K_i = 34 nM) for a subset of muscarinic receptors present in rat cerebral cortex, presumably similar to the cardiac M_2 subtype (37, 38). However, there is evidence that the low affinity AF-DX 116 binding site might be a composite of more than one receptor subtype (38, 39). Moreover, the pK_i of the low affinity component of AF-DX 116 competition against [^{3}H]

TABLE 5

Competition for [^{3}H]NMS binding in cell aggregates of rat cerebral cortex by muscarinic antagonists

Cell aggregates were prepared from rat brain cortex and incubated in KH buffer in the presence of 0.2 nM [^{3}H]NMS and varying concentrations of the different antagonists for 90 min at 37°. Nonspecific binding was determined in the presence of 2 μM atropine. Data are shown as the mean ± standard error of *n* independent experiments. See Table 2 for abbreviations.

Antagonist	*n*	pK_h	pK_l	R_h	n_H
				%	
Pirenzepine	6	8.40 ± 0.22	6.43 ± 0.13	49 ± 9	0.6 ± 0.05
Telenzepine	3	8.70 ± 0.06	7.30 ± 0.32	55 ± 8	0.6 ± 0.07
AF-DX 116	7	7.35 ± 0.05	6.02 ± 0.06	45 ± 6	0.7 ± 0.02
HHSiD	6	7.55 ± 0.06		100	0.9 ± 0.02
4-DAMP	5	8.92 ± 0.07		100	0.8 ± 0.1
Atropine	4	9.08 ± 0.08		100	1.0 ± 0.02

TABLE 6

Competition for [^{3}H]telenzepine binding in cell aggregates from rat cerebral cortex by muscarinic antagonists

Cell aggregates were prepared as described in Experimental Procedures and were incubated in the presence of 1 nM [^{3}H]telenzepine and varying concentrations of the antagonists for 3 hr at 37° in KH buffer. Nonspecific binding was determined in the presence of 2 μM atropine. Data are shown as the mean ± standard error of *n* independent experiments.

Antagonist	*n*	pK_i	n_H
Pirenzepine	4	7.60 ± 0.06	1.0 ± 0.03
Telenzepine	3	8.82 ± 0.08	1.0 ± 0.01
AF-DX 116	6	5.90 ± 0.13	0.9 ± 0.04
HHSiD	5	7.52 ± 0.05	1.0 ± 0.02
4-DAMP	5	8.40 ± 0.05	1.0 ± 0.04

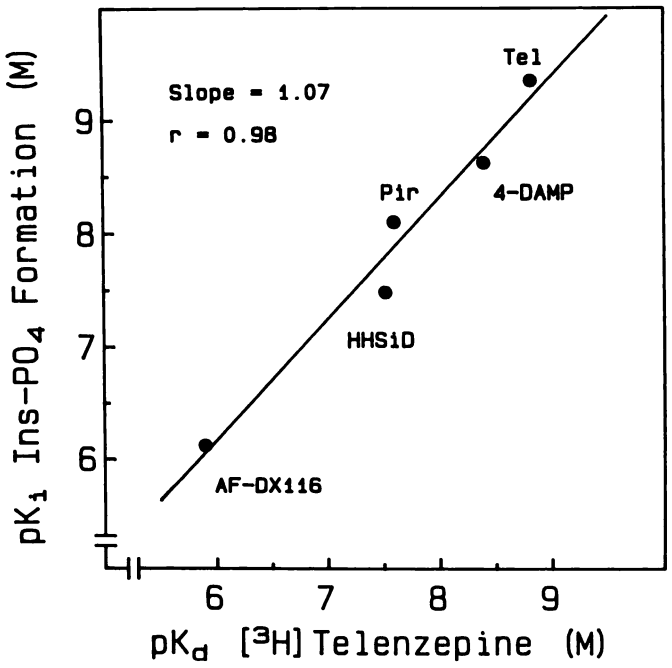

Fig. 11. Relationship between the equilibrium dissociation constants of muscarinic antagonists in inhibiting carbamylcholine-induced [^{3}H]inositol phosphates formation and [^{3}H]telenzepine binding. Data were taken from Tables 2 and 5. *Ins-PO$_4$*, inositol phosphates. Pir, pirenzepine; *Tel*, telenzepine.

NMS binding (6.02 ± 0.06) is in close agreement with the one detected in [^{3}H]telenzepine binding assays (5.9 ± 1.13), the pK_b estimated from the PI response induced by carbamylcholine (6.12 ± 0.28), and the pA_2 value from its antagonism of oxotremorine-M (6.23 ± 0.10). Thus, these data indicate that AF-DX 116 can differentiate at least two subsets of muscarinic receptors in cortical cell aggregates in binding assays and only one site with low affinity in the activation of PI metabolism by carbamylcholine. This finding suggests that in the rat cerebral cortex, M_2 receptors do not activate the PI response. This notion is supported by gene expression studies, where it has been demonstrated that M_2 receptors are mainly coupled to inhibition of adenylate cyclase (16).

The biphasic profile obtained with the M_1-selective antagonists pirenzepine and telenzepine for their ability to inhibit the PI response induced by muscarinic agonists was in sharp contrast to the results obtained using atropine, 4-DAMP, HHSiD, and AF-DX 116. The inhibition curves produced by these two antagonists were biphasic when PI metabolism was activated by either acetylcholine, oxotremorine-M, or carbamylcholine, and the data from these curves could be fitted to a two-site model significantly better than to a one-site model. The resulting pK_b values for the high affinity component of pirenzepine inhibition using these three agonists were virtually identical, and they corresponded closely to the high affinity pK_i determined in [^{3}H]NMS binding assays and the pK_i obtained in [^{3}H]telenzepine binding assays. Similar results were obtained when the activation of the PI response by carbamylcholine was inhibited by telenzepine. The A-S plot of the antagonism by pirenzepine of the activation of PI metabolism by oxotremorine-M estimated a pA_2 very close to the pK_b and pK_i of the high affinity component of pirenzepine inhibition. In this regard the proportion of the PI response inhibited with high affinity by either pirenzepine or telenzepine was consistently found to correspond to two thirds of the total response, regardless of the agonist used. These data argue strongly in favor of the classification of this high affinity component, as measured in PI assays, as being mediated by an M_1 receptor subtype.

However, the A-S plots for pirenzepine were linear up to 1 μM but showed a marked deviation from linearity at higher concentrations. One possible interpretation of these data is the presence of cooperativity in the antagonism by pirenzepine. The results from the additivity of the dose ratio also showed that at high concentrations pirenzepine and telenzepine antagonism seemed to deviate from a simple competitive interaction. Similar findings have been reported earlier for the antagonism by pirenzepine of the activation of prejunctional muscarinic receptors by McN-A-343 (40). However, there were no signs of cooperativity when carbamylcholine was used as an agonist, suggesting that this anomalous interaction was not related to pirenzepine but more likely to the allosteric properties of McN-A-343 (39). Moreover, pirenzepine does not alter the dissociation rate of [^{3}H]quinuclidinylbenzilate in the whole brain (41), and we have also found that neither pirenzepine nor telenzepine altered the dissociation rate of [^{3}H]NMS induced by atropine in rat cerebral cortex cell aggregates (data not shown). The presence of such an effect of an antagonist on dissociation kinetics is a hallmark for the presence of cooperative interaction (42). These results suggest that allosterism does not represent a major mechanism for the interaction of pirenzepine and muscarinic receptors. Furthermore, the fact that the inhibition by pirenzepine of the effects of a single concentration of carbamylcholine, as well as the linearity of the A-S plot after alkylation of the low affinity binding sites of this antagonist by PBCM, indicates that there is a relationship between the interaction of pirenzepine with multiple receptor subtypes and its biphasic inhibition of PI hydrolysis and excludes a contribution of an allosteric effect. It should also be pointed out that our finding of an identical value for the K_b of the high and low affinity components of pirenzepine in inhibiting the response to three different agonists (Table 3) does not conform to an allosteric mechanism of inhibition (43). Taken together, these data suggest that the observation of a less than additive dose ratio of pirenzepine and atropine cannot be unambiguously considered as evidence of cooperative interactions of pirenzepine with M_1 receptors, which result in its anomalous inhibitory profile.

Another possible explanation of the data is that the biphasic behavior of pirenzepine and telenzepine is only apparent and might be due to an interaction of muscarinic agonists with two receptor conformations. This interpretation is not likely for

two reasons. First, the Hill coefficients of the concentration-response curves of the agonists in stimulating PI hydrolysis were close to unity. Our results in this respect differ from those of others who have found markedly biphasic dose-response curves for the activation of PI metabolism by carbamylcholine in rat striatum cell aggregates (28). Second, if this interpretation is valid, any muscarinic antagonists should have behaved in a manner similar to pirenzepine and telenzepine, which is not the case.

The most parsimonious explanation of these findings is that the response being measured is elicited by a heterogeneous population of receptors that show different affinities for pirenzepine and telenzepine, as suggested by the nonlinear A-S plot. This possibility is supported by our finding of a linear A-S plot after the selective alkylation of the receptors that show low affinity for pirenzepine (Fig. 10) and also the evidence of monophasic curves for the inhibition by pirenzepine of the response to carbamylcholine after this treatment (Fig. 9). In the case of receptor heterogeneity, however, the A-S plot from control cells would show a transient change in slope and would later resume an upward trend. Unfortunately, we could not obtain this evidence, because this would require the assay of very high concentrations of oxotremorine-M, which produce less than maximal response, most likely due to nonspecific effects on the viability of the cell aggregate preparation (data not shown).

As to the identity of the muscarinic receptor subtypes that activate PI metabolism in rat brain cortex, M_1 receptors are certainly involved, due to the close correspondence of the inhibition constants of the series of antagonists tested in inhibiting ligand binding to M_1 receptors and their potency at the high affinity site in inhibiting the PI response. In addition, the pK_b of pirenzepine for its high affinity site in inhibiting PI is very close to that obtained in murine B82 cells transfected with the m1 receptor gene (17). Cell transfection studies have demonstrated that muscarinic receptor subtypes that could be coupled to PI metabolism also include the products of the m3 and m5 receptor genes (10, 11, 16, 44). Although the m5 receptor exhibits a low affinity for pirenzepine, it is unlikely that it represents the low affinity pirenzepine component in the inhibition of PI metabolism, because the m5 transcript has not been found in rat cerebral cortex (46). A more likely candidate is the pharmacologically defined M_3 muscarinic receptor (which is the product of the m3 gene). Evidence for this proposal is severalfold. First, *in situ* hybridization studies have demonstrated the abundance of m3 mRNA in rat brain cortex (13–15). Second, the low affinity equilibrium dissociation constant of pirenzepine in inhibiting the PI response (263 nM) corresponds well to that of this antagonist in antagonizing PI hydrolysis activated by muscarinic receptors pharmacologically classified as M_3 in glandular tissue (124 nM) (3, 45), SK-N-SH human neutorblastoma cells (234 nM) (35), and human astrocytoma 1321 N1 cells (170 nM) (47). The main caveat to this conclusion derives from functional studies that have consistently found that muscarinic agonists activate PI metabolism with potencies at least 10-fold higher in glandular tissue (3, 45, 48), human astrocytoma 1321N1 cells (47), human neuroblastoma SK-N-SH cells (35), and cells transfected with the recombinant m3 DNA (16, 44), when compared with the potency of the same agonists to activate PI metabolism through M_1 receptors. However, it has been shown that in SK-N-SH cells the high potency of muscarinic agonists in stimulating PI hydrolysis is due to the presence of a large receptor reserve, probably reflecting a more efficient receptor-effector coupling (35). This should not necessarily be the case for brain M_3 receptors.

The finding of monophasic inhibition curves for pirenzepine when the full agonist methacholine and the partial agonist bethanechol were used to activate PI metabolism might be taken to suggest that these agonists differ in their efficacy to activate M_1 and M_3 receptors. The resulting A-S plot for pirenzepine in antagonizing methacholine was linear up to 1 μM, with a pA_2 value for pirenzepine that corresponded closely to its affinity for M_1 receptors, suggesting that methacholine is only able to stimulate PI metabolism in rat brain cortex mainly by activating the M_1 receptor subtype. Unfortunately, it was not possible to investigate the linearity of the dose ratio of pirenzepine at concentrations similar to those assayed with oxotremorine-M, because methacholine beyond 50 mM induced a depression of the maximal PI response. Further investigation is needed to demonstrate that methacholine and bethanechol differ in their efficacy or potency to activate the PI response, under conditions whereby the two functional components could be resolved.

In summary, our results provide convincing evidence for the involvement of more than one muscarinic receptor subtype in the activation of PI metabolism in rat cerebral cortex, these subtypes being distinguished by pirenzepine and telenzepine. These data give strong experimental support to the hypothesis of heterogeneity of PI-coupled muscarinic receptors, which was put forward in earlier studies (25, 26), and identify the muscarinic receptor subtypes involved. A detailed examination of the coupling of the different muscarinic receptor subtypes to the PI effector system in other brain areas is in order, in light of our findings. These aspects are of particular relevance to our understanding of the physiological significance of muscarinic receptor subtypes in cerebral functions under normal and pathological conditions.

Acknowledgments

The authors would like to thank Mr. Michael Gentry and Mr. Walter Thompson for their invaluable assistance.

References

1. Hammer, R., C. P. Berrie, N. J. M. Birdsall, A. S. V. Burgen, and E. C. Hulme. Pirenzepine distinguishes between different subclasses of muscarinic receptors. *Nature (Lond.)* **283**:90–92 (1980).
2. Hammer, R., and A. Giachetti. Muscarinic receptor subtypes: M_1 and M_2 biochemical and functional characterization. *Life Sci.* **31**:2991–2998 (1982).
3. Gil, D. W., and B. Wolfe. Pirenzepine distinguishes between muscarinic receptor-mediated phosphoinositide breakdown and inhibition of adenylate cyclase. *J. Pharmacol. Exp. Ther.* **232**:608–616 (1984).
4. McKinney, M., S. Stenstrom, and E. Richelson. Muscarinic responses and binding in a murine neuroblastoma clone (N1E-115): mediation of separate resposnes by high affinity and low affinity agonist-receptor conformations. *Mol. Pharmacol.* **27**:223–235 (1985).
5. McKinney, M., D. Anderson, and L. Vella-Rountree. Different agonist-receptor active conformations for brain M1 and M2 muscarinic receptors that are separately coupled to two biochemical effector systems. *Mol. Pharmacol.* **35**:39–47 (1989).
6. Doods, H. N., M.-J. Mathy, D. Davidesko, K. J. van Charldorp, A. de Jonge, and P. A. van Zwieten. Selectivity of muscarinic antagonists in radioligand and *in vivo* experiments for the putative M_1, M_2 and M_3 receptors. *J. Pharmacol. Exp. Ther.* **242**:257–262 (1987).
7. Kubo, T., K. Fukuda, A. Mikami, A. Maeda, H. Takahashi, M. Mishina, T. Haga, A. Ichiyama, K. Kangawa, M. Kojima, H. Matsuo, T. Hirose, and S. Numa. Cloning, sequencing and expression of complementary DNA encoding the muscarinic acetylcholine receptor. *Nature (Lond.)* **323**:411–416 (1986).
8. Bonner, T. I., N. J. Buckley, A. C. Young, and M. R. Brann. Identification of a family of muscarine acetylcholine receptor genes. *Science (Wash. D. C.)* **237**:527–532 (1987).

9. Peralta, E. G., A. Ashkenazi, J. W. Winslow, D. H. Smith, J. Ramachandran, and D. J. Capon. Distinct primary structures, ligand-binding properties and tissue-specific expression of four human muscarinic acetylcholine receptors. *EMBO J.* **6**:3923–3929 (1987).
10. Bonner, T. I., A. C. Young, M. R. Brann, and N. J. Buckley. Cloning and expression of the human and rat m5 muscarinic acetylcholine receptor genes. *Neuron* **1**:403–410 (1988).
11. Liao, C.-F., A. P. N. Themmen, R. Joho, C. Barberis, M. Birnbaumer, and L. Birnbaumer. Molecular cloning and expression of a fifth muscarinic acetylcholine receptor. *J. Biol. Chem.* **264**:7328–7337 (1989).
12. Buckley, N. J., T. I. Bonner, C. M. Buckley, and M. R. Brann. Antagonist binding properties of five cloned muscarinic receptors expressed in CHO-K1 cells. *Mol. Pharmacol.* **35**:469–476 (1989).
13. Brann, M. R., N. J. Buckley, and T. I. Bonner. The striatum and cerebral cortex express different muscarinic receptor mRNAs. *FEBS Lett.* **230**:90–94 (1988).
14. Buckley, N. J., T. I. Bonner, and M. R. Brann. Localization of a family of muscarinic receptor mRNAs in rat brain. *J. Neurosci.* **8**:4646–4652 (1988).
15. Maeda, A., T. Kubo, M. Masayoshi, and S. Numa. Tissue distribution of mRNAs encoding muscarinic acetylcholine receptor subtypes. *FEBS Lett.* **239**:339–342 (1988).
16. Peralta, E. G., A. Ashkenazi, J. W. Winslow, J. Ramaschandran, and D. J. Capon. Differential regulation of PI hydrolysis and adenylyl cyclase by muscarinic receptor subtypes. *Nature (Lond.)* **334**:434–437 (1988).
17. Lai, J., L. Nei, W. R. Roeske, F. Z. Chung, H. I. Yamamura, and J. C. Venter. The cloned murine M_1 muscarinic receptor is associated with the hydrolysis of phosphatidylinositols in transfected murine B82 cells. *Life Sci.* **42**:2489–2502 (1988).
18. Shapiro, A. R., N. M. Scherer, B. A. Habecker, E. M. Subers, and N. Nathanson. Isolation, sequence, and functional expression of the mouse M1 muscarinic acetylcholine receptor. *J. Biol. Chem.* **263**:18397–18403 (1988).
19. Gonzales, R. A., and F. T. Crews. Characterization of the cholinergic stimulation of phosphoinositide hydrolysis in rat brain slices. *J. Neurosci.* **4**:3120-3127 (1984).
20. Brown, E., D. A. Kendall, and S. R. Nahorski. Inositol phospholipid hydrolysis in rat cerebral cortical slices. I. Receptor characterization. *J. Neurochem.* **42**:1379–1387 (1984).
21. Fisher, K. S., J. C. Figueiredo, and R. T. Bartus. Differential stimulation of inositol phospholipid turnover in brain by analogs of oxotremorine. *J. Neurochem.* **43**:1171–1179 (1984).
22. Fisher, K. S., and R. T. Bartus. Regional differences in the coupling of muscarinic receptors to inositol phospholipid hydrolysis in guinea pig brain. *J. Neurochem.* **45**:1085–1095 (1985).
23. Waelbroeck, M., M. Gillard, P. Robberecht, and J. Christophe. Muscarine receptor heterogeneity in rat central nervous system. I. Binding of four selective antagonists to three muscarinic receptor subclasses. A comparison with M2 cardiac muscarinic receptors of the C type. *Mol. Pharmacol.* **32**:91–99 (1987).
24. Gillard, M., M. Waelbroeck, and J. Christophe. Muscarinic receptor heterogeneity in rat central nervous system. II. Brain receptors labeled by [^{3}H] oxotremorine-M correspond to heterogeneous M2 receptors with very high affinity for agonists. *Mol. Pharmacol.* **32**:100–108 (1987).
25. Lazareno, S., D. A. Kendall, and S. R. Nahorski. Pirenzepine indicates heterogeneity of muscarinic receptors linked to cerebral inositol phospholipid metabolism. *Neuropharmacology* **24**:593–595 (1985).
26. Rooney, T. A., and S. R. Nahorski. Regional characterization of agonist- and depolarization-induced phosphoinositide hydrolysis in rat brain. *J. Pharmacol. Exp. Ther.* **239**:873–880 (1986).
27. Kunysz, E. L., A. D. Michel, and R. L. Whiting. Functional and direct binding studies using subtype selective muscarinic receptor antagonists. *Br. J. Pharmacol.* **93**:491–500 (1988).
28. Monsma, F. J., L. G. Abood, and W. Hoss. Inhibition of phosphoinositide turnover by selective muscarinic antagonists in the rat striatum. *Biochem. Pharmacol.* **37**:2437–2443 (1988).
29. Honegger, P., and E. Richelson. Biochemical differentiation of mechanically dissociated mammalian brain in aggregating cell culture. *Brain Res.* **109**:335–354 (1976).
30. Lee, J.-H., and E. E. El-Fakahany. [^{3}H]*N*-Methylscopolamine binding to muscarinic receptors in intact adult rat brain cell aggregates. *Biochem. Pharmacol.* **34**:4299–4303 (1985).
31. Berridge, M. J., C. P. Downes, and M. R. Hanley. Lithium amplifies agonist-dependent phosphatidylinositol responses in brain and salivary glands. *Biochem. J.* **206**:587–595 (1982).
32. Arunlakshana, O., and H. O. Schild. Some quantitative uses of drug antagonists. *Br. J. Pharmacol.* **14**:48–58 (1959).
33. Eglen, R. M., and R. L. Whiting. Problems associated with the application of the Cheng-Prusoff relationship to estimate atropine affinity constants using functional tissue responses. *Life Sci.* **44**:81–94 (1989).
34. Munson, P. J., and D. Rodbard. LIGAND: a versatile computerized approach for the characterization of ligand binding systems. *Anal. Biochem.* **107**:220–239 (1980).
35. Fisher, S. K., and R. M. Snider. Differential receptor occupancy requirements for muscarinic cholinergic stimulation of inositol lipid hydrolysis in brain and in neuroblastomas. *Mol. Pharmacol.* **32**:81–90 (1987).
36. Furchgott, R. F., and P. Burstyn. Comparison of dissociation constants and of relative efficacies of selected agonists acting on parasympathetic receptors. *Ann. N. Y. Acad. Sci.* **139**:882–899 (1967).
37. Wang, J. X., W. R. Roeske, K. Gulya, W. Wang, and H. I. Yamamura. [^{3}H] AF-DX 116 labels subsets of muscarinic cholinergic receptors in rat brain and heart. *Life Sci.* **41**:1751–1760 (1986).
38. Giraldo, E., R. Hammer, and H. Ladinsky. Distribution of muscarinic receptor subtypes in rat brain as determined in binding studies with AF-DX 116 and pirenzepine. *Life Sci.* **40**:833–840 (1987).
39. Giraldo, E., D. Monferini, H. Ladinsky, and R. Hammer. Muscarinic receptor heterogeneity in guinea pig intestinal smooth muscle: binding studies with AF-DX 116. *Eur. J. Pharmacol.* **141**:475–477 (1987).
40. Choo, L. K., F. Mitchelson, and Y. M. Vong. The interaction of McN-A-343 with pirenzepine and other selective muscarine receptor antagonists at a prejunctional muscarine receptor. *Naunyn-Schmiedeberg's Arch. Pharmacol.* **328**:430–438 (1985).
41. El-Fakahany, E. E., C. L. Cioffi, M. M. Abdellatif, and M. M. Miller. Competitive interaction of pirenzepine with rat brain muscarinic receptors. *Eur. J. Pharmacol.* **131**:237–247 (1986).
42. Lee, N. H., and E. E. El-Fakahany. Influence of ligand choice on the apparent binding profile of gallamine to cardiac muscarinic receptors: identification of three main types of gallamine-muscarinic receptor interactions. *J. Pharmacol. Exp. Ther.* **246**:829–838 (1988).
43. Kenakin, T., and C. Boselli. Pharmacologic discrimination between receptor heterogeneity and allosteric interaction: resultant analysis of gallamine and pirenzepine antagonism of muscarinic responses in rat trachea. *J. Pharmacol. Exp. Ther.* **250**:944–952 (1989).
44. Bujo, H., J. Nakai, T. Kubo, K. Fukuda, I. Akiba, A. Maeda, M. Mishina, and S. Numa. Different sensitivities to agonist of muscarinic acetylcholine receptor subtypes. *FEBS Lett.* **240**:95–100 (1988).
45. Ek, B., and S. Nahorski. Muscarinic receptor coupling to inositol phospholipid metabolism in guinea-pig cerebral cortex, parotid gland and ileal smooth muscle. *Biochem. Pharmacol.* **37**:4461–4467 (1988).
46. Weiner, D. M., and M. R. Brann. Distribution of m1–m5 muscarinic receptor mRNAs in rat brain. *Trends Pharmacol. Sci.* (suppl.) 115 (1989).
47. Kunysz, E. A., A. D. Michel, R. L. Whiting, and K. Woods. The human astrocytoma cell line 1321 N1 contains M_3-glandular type muscarinic receptors linked to phosphoinositide turnover. *Br. J. Pharmacol.* **96**:271–278 (1989).
48. Dehaye, J.-P., A. Marino, Y. Soukias, P. Poloczek, J. Winand, and J. Christophe. Functional characterization of muscarinic receptors in rat parotid acini. *Eur. J. Pharmacol.* **151**:427–434 (1988).

Send reprint requests to: Esam E. El-Fakahany, Ph.D., Department of Pharmacology and Toxicology, University of Maryland School of Pharmacy, 20 N. Pine St., Baltimore, MD 21201.